Semiautomatic Regional Segmentation to Measure Orbital Fat Volumes in Thyroid-Associated Ophthalmopathy

A Validation Study

M. COMERCI[1], A. ELEFANTE[2], D. STRIANESE[3], R. SENESE[2], P. BONAVOLONTÀ[3], B. ALFANO[1], G. BONAVOLONTÀ[3], A. BRUNETTI[1,2]

[1] Biostructure and Bioimaging Institute, National Research Council; Naples, Italy
[2] Department of Advanced Biomedical Sciences, Neuroradiology, "Federico II" University; Naples, Italy
[3] Department of Neurosciences, Reproductive Sciences and Odontostomatology, "Federico II" University; Naples, Italy

Key words: semiautomatic numeric segmentation, orbital quadrant definition, regional orbital fat quantification, Graves' orbitopathy, MRI segmentation, validation

SUMMARY – *This study was designed to validate a novel semi-automated segmentation method to measure regional intra-orbital fat tissue volume in Graves' ophthalmopathy. Twenty-four orbits from 12 patients with Graves' ophthalmopathy, 24 orbits from 12 controls, ten orbits from five MRI study simulations and two orbits from a digital model were used. Following manual region of interest definition of the orbital volumes performed by two operators with different levels of expertise, an automated procedure calculated intra-orbital fat tissue volumes (global and regional, with automated definition of four quadrants). In patients with Graves' disease, clinical activity score and degree of exophthalmos were measured and correlated with intra-orbital fat volumes. Operator performance was evaluated and statistical analysis of the measurements was performed. Accurate intra-orbital fat volume measurements were obtained with coefficients of variation below 5%. The mean operator difference in total fat volume measurements was 0.56%. Patients had significantly higher intra-orbital fat volumes than controls ($p<0.001$ using Student's t test). Fat volumes and clinical score were significantly correlated ($p<0.001$). The semi-automated method described here can provide accurate, reproducible intra-orbital fat measurements with low inter-operator variation and good correlation with clinical data.*

Introduction

Segmentation procedures for normal and abnormal tissue classification can be of value in the assessment of disease extent and measurement of disease-associated changes over time. While several segmentation procedures are currently available for brain structures, only a few applications have been described for extra-cerebral tissue segmentation [1-5]. In particular, extra-ocular tissue segmentation could be useful for the evaluation of Graves' ophthalmopathy, an autoimmune disorder caused by auto-reactive CD4 T lymphocytes recognizing a similar antigen to thyroid and orbital tissue, causing edematous expansion of the extra-ocular muscles and increased volume of the orbital tissue [6-11].

Most currently available segmentation procedures for orbital tissue measurements are heavily time-consuming since they are based on manual segmentation [1-5]. Moreover, none involves automatic quadrant separation, which could be useful for surgical planning [12]. Therefore, we developed and tested an MRI-based computer-assisted method for global and regional segmentation of orbital fat using a digital brain phantom [13]. The phantom was used by two operators with different levels of expertise. We also evaluated the correlation between

intra-orbital fat tissue and the degree of exophthalmos and the clinical activity score (CAS) in patients with dysthyroid ophthalmopathy.

Materials and Methods

MRI protocol

MRI studies were acquired at 1.5 Tesla (Philips Intera, Philips Medical Systems, Best, The Netherlands). Transverse single echo T1-w conventional spin echo (CSE) (TR 600 ms, TE 15ms) and double echo T2-w/PD-w CSE (TR 2200ms, TE 15/90 ms) sequences with the same geometry (field of view (FOV) 240 mm, slice thickness 4 mm, matrix 256×256) were obtained on both normal controls and patients. Simulations of MRI studies were also performed.

Patients, controls and phantoms

The study was performed in compliance with the guidelines of the Declaration of Helsinki. Twelve patients (ten women and two men, mean age 47.2 years, standard deviation (SD) 10.4 years) with Graves' ophthalmopathy of median disease duration 24 months, and 12 controls (ten women, two men, mean age 44.1 years, SD 7.1 years) were included in the study. All participants provided informed consent to the procedure. The degree of exophthalmos (mm) was determined with reference to the interzygomatic line on axial MRI images. In patients, the clinical activity score (CAS) – taking into account pain, eyelid, erythema or edema, conjunctival hyperemia and chemosis – was assessed by thorough clinical examination.

Two operators (a neuroradiologist and an ophthalmologist) made a pre-selection of orbital regions on MRI images for subsequent segmentation of orbital structures. This pre-selection consisted in manually creating a region of interest (ROI) comprising all orbital tissues, performed slice by slice on the transverse slices of the T1-w images. The aim was to divide extra-orbital from intra-orbital tissues.

A set of five brain MRI study simulations, based on a digital phantom described in Alfano et al. [13], was used for the validation study. This phantom was useful since it comprises most of the extracranial tissues, such as fat, muscle, bone and vitreous useful to validate our method. Moreover the MRI simulation includes acquisition aspects that make the validation more challenging. The phantom model [13] was used as a reference to evaluate segmentation accuracy.

MRI processing

The scans and simulations were segmented with the algorithm described by Alfano et al. [14]. Briefly, the software calculates relaxation rates (R1, the inverse of the T1 relaxation time, and R2, the inverse of the T2 relaxation time) and proton density from the MRI acquisitions (a conventional spin echo T1-w single echo and a conventional spin echo PD-w/T2-w double echo are required to perform this calculation), pre-processes them to reduce noise and partial volume effects and then recognizes the different tissues according to the rates and proton density values. The segmentation software automatically recognizes muscle, fat and vitreous body, among other tissues. Two three-dimensional regions of interest (ROIs), including the orbital cavities, were defined for each scan and MRI simulation using a slice-by-slice manual definition, described earlier, and automated three-dimensional fitting and regularization. An expert operator defined the two ROIs on the phantom model to obtain the reference volumes for the validation.

The ROIs were automatically subdivided into four quadrants (superior, [S], lateral, [L], inferior, [I] and medial, [M]) using software developed in-house. The volumes of interest were obtained by intersecting the segmented tissues with the above sub-ROIs. A sample of ROIs is shown in Figure 1.

To define the four quadrants, the software uses three reference points automatically calculated from segmentation data: the two centers of mass of the vitreous bodies and a point (named X) located 1.3 cm behind the substantia nigra and red nucleus center of mass. This distance was chosen empirically to represent the virtual intersection of the prolongation of the optical tracts.

These points define a plane, taken as reference for the quadrants. Ideally this is the plane in which the eyes and the optical tracts lie. Then the quadrants are defined starting from this plane as explained below.

The software procedure first defines a plane a, passing through these three points and including the path of the intra-orbital optical nerves. Subsequently, the software defines two additional orthogonal planes for each eye, intersecting along the axis defined by the center

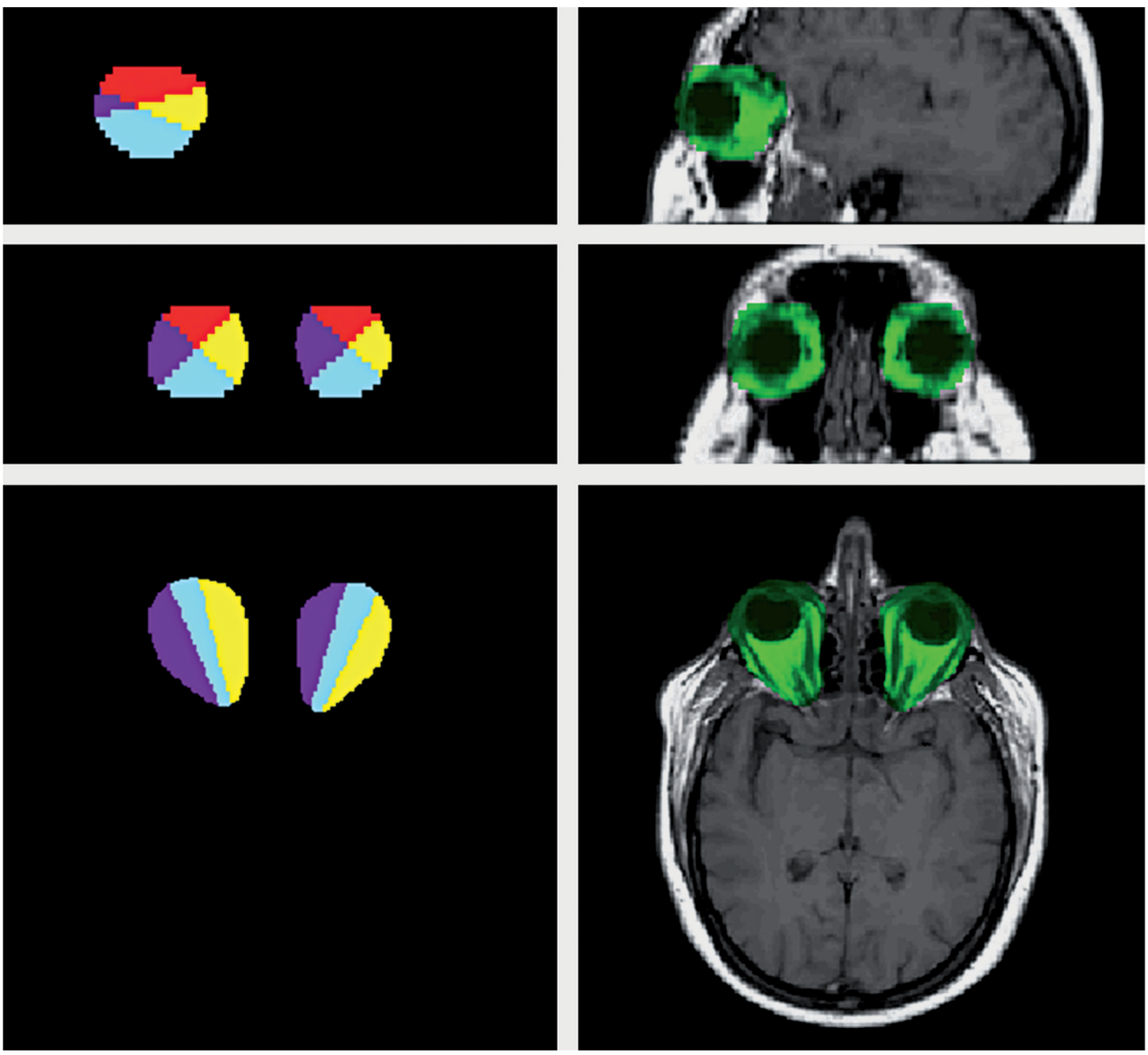

Figure 1 Example of manually selected ROIs. Left, top to bottom: sagittal, coronal and transversal orthogonal cuts of the 3D ROIs, divided into the four quadrants. Right, top to bottom: sagittal, coronal and transversal orthogonal cuts of the 3D ROIs, overlaid on a T1-w image using a simple channel masking method, showing ROI voxels in green.

of mass of the eye and the point X, with 45° tilting compared with plane a. These four planes define the four quadrants for each eye. Finally, the volumes of fat, muscle and vitreous bodies are calculated for each quadrant of each eye accordingly.

This is performed by the automated segmentation method that separates muscle, fat, bone and vitreous. Data processing requires about ten minutes per study, to be summed to the manual ROI definition.

Validation data

To validate the segmentation method, calculations were performed for each patient, for each simulation and for each operator. Mean value, SD and coefficient of variation (CV) were calculated. Mean values were compared with the reference values measured on the model.

To assess the operator variability, the percentage difference between orbital fat measurements was calculated for each orbit and for

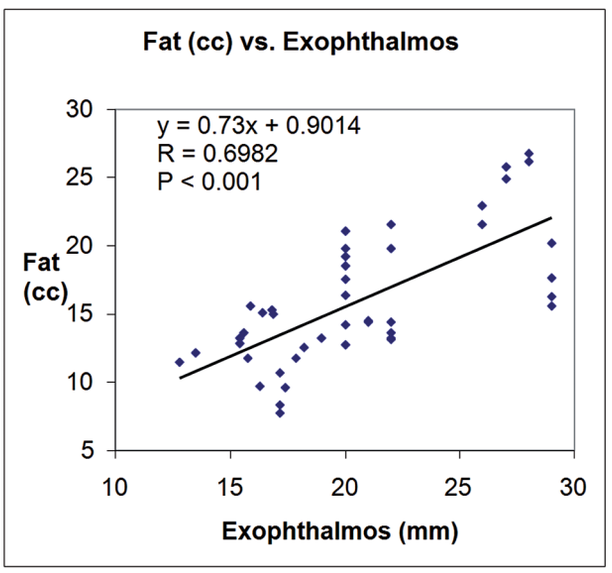

Figure 2 Plot of orbital fat volume (cc) versus exophthalmos (mm) along with the linear fitting data.

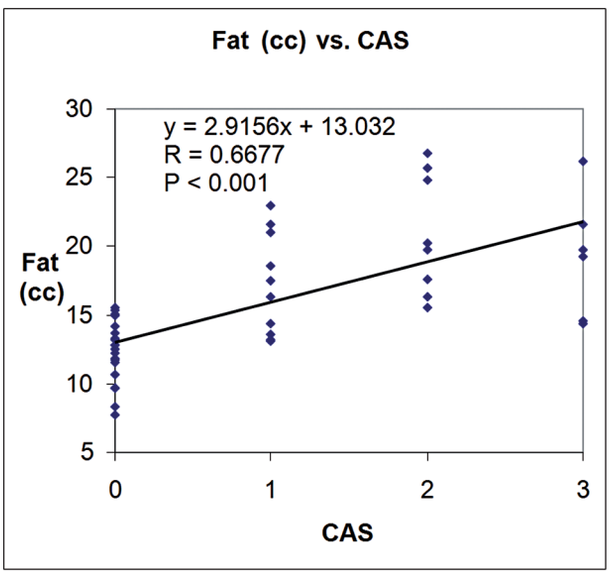

Figure 3 Plot of orbital fat volume (cc) versus CAS, along with the linear fitting data.

all 12 patients, 12 controls and five simulations. The mean values and the SDs were then calculated. To assess the differences between patients and controls, mean value and SDs of total fat volume for the patient orbits, control orbits and simulated orbits were calculated. One-sided unpaired t tests were performed to compare the control and patient volume measurements for each quadrant and the whole orbit made by the two operators and the means of the operator values. Finally, the total fat volumes for patients and controls were linearly correlated with exophthalmos and CAS indices to give the coefficients of linear fitting, the correlation coefficients and the p values. A confidence threshold of 0.01 was used.

Table 1 Fat volumes (cc) in the reference study versus measured values.

	Reference	*Mean ± SD*
Total	13.67	11.48±0.56
Superior	3.86	3.21±0.24
Lateral	2.20	1.88±0.09
Inferior	4.73	4.14±0.40
Medial	2.88	2.25±0.13

Results

Mean exophthalmos was 23.92 mm ± 3.74 mm in patients and 16.84 mm ± 1.82 mm in controls. Mean CAS was 1.83 mm ± 0.81 mm in patients. Table 1 reports the fat volumes of quadrants and orbits obtained from the model and the simulation. The first column shows the reference volumes as defined by the model. Mean values and SDs of the fat volumes as measured on the 20 orbits (five simulations × two orbits × two operators) are also reported in Table 1. The mean percentage operator difference in total fat volume measures (58 measures for each operator) was 0.56 ± 4.91%. The mean orbital fat volume was 18.95 cc ± 4.27 cc for the patients, 12.34 cc ± 2.25 cc for the controls and 11.48 cc ± 0.47 cc for the simulations. The p values from one-sided unpaired t tests comparing the fat volumes for controls and patients assessed by operator 1 and operator 2 and the mean be-

Table 2 Fat volume (cc) t tests between controls and patients for each operator and for the mean operator.

	Operator 1					*Operator 2*					*Mean of operators*				
	S	L	I	M	Tot	S	L	I	M	Tot	S	L	I	M	Tot
Patients vs. NC	0.007	0.000	0.000	0.000	0.000	0.026	0.000	0.000	0.000	0.000	0.013	0.000	0.000	0.000	0.000

tween the two operators for each quadrant and whole orbit are reported in Table 2. Figures 2 and 3 show the linear fitting between total fat volume (cc) and Exophthalmos (mm) and CAS, respectively, along with the linear fitting equation, the correlation coefficient and the *p* value.

Discussion and Conclusions

The clinical symptoms and signs of Graves orbitopathy (GO) can be explained mechanically by the discrepancy between the increased volume of the swollen orbital tissues and the fixed volume of the bony orbit. The expanded orbital tissues displace the globe forward and impede venous outflow from the orbit. These changes, combined with the local production of cytokines and other mediators of inflammation, result in pain, proptosis, peri-orbital edema, conjunctival injection, and chemosis. Computed tomographic scans show that most patients with GO have enlargement of both the orbital fat compartments and the extra-ocular muscles and that others appear to have involvement of only adipose tissue or extra-ocular muscle. Therefore Graves' orbitopathy appears to be a multifactorial disease rather than a unique entity.

It is well known that the extra-ocular muscles (EOM) are enlarged in dysthyroid ophthalmopathy leading to proptosis and diplopia. This can be easily observed clinically [18,28] or by imaging techniques as ultrasonography [19], x-ray computed tomography (CT) [20,28] and magnetic resonance imaging (MRI) [21].

Increased orbital tissue volume, leading to exophthalmos, could also be due to expansion of the orbital fatty tissue. Quantitative evaluation of orbital fat volume in dysthyroid ophthalmopathy has been done with CT [22]. MRI studies of dysthyroid ophthalmopathy patients' characteristics concluded that in absolute values the increment of orbital fat volume was larger than that of all EOM together, implying that orbital fat volume change is an important contributor to exophthalmos [23]. In addition, severity of proptosis appears to be more closely related to the orbital adipose and connective tissue volume than to muscle volume. This expanded adipose tissue volume results from both hyaluronic acid-related edema and the emergence of a population of newly differentiated fat cells within these tissues [24,25].

Compressive optic neuropathy and exposure keratopathy are classical indications for orbital decompression surgery to treat thyroid-associated ophthalmopathy. Recently, the therapeutic value of orbital decompression has been extended to cosmetic requirements, the entity of congestive orbitopathy, ocular hypertension and hormonal resistance. Orbital decompression may be performed using a wide spectrum of surgical approaches and procedures, but the criteria for selection of the appropriate surgical technique have not been well defined. Hence, the surgical technique has largely been selected by surgeon or institutional preference rather than specific patient characteristics. However, in recent years, to improve the safe and efficacy of orbital decompressions, there is a general tendency to design graded decompression plans and find modified areas of bone and fat removal. The areas of bone removal are different combinations of medial, inferior and deep lateral wall decompression. There have also been technical advances in cosmetic incisions such as trans-conjunctival, eyelid crease or endoscopic access. Removing peri-orbital fat may be performed alone [26,27] or as a supplement to bony decompression. The amount removed amount and indications should be strictly regulated and an individual operative project devised. For these reasons we design a four quadrant scheme of division of the orbit to improve the understanding of orbital fat distribution in patients with dysthyroid orbitopathy. This four-quadrant scheme may allow surgeons a preoperative evaluation of the amount of fat to be removed to achieve good results. Eventually, the division of the orbit may constitute a relevant anatomical landmark since each quadrant contains different critical structures such as nerve, muscle and vessels, which should be included in the preoperative evaluation together with fat removal. Furthermore, given the increasing interest in surgical approaches for fat removal to decrease the amount of exophthalmos, regional assessment of intra-orbital fat by dividing the orbits into four quadrants could be useful for more accurate surgical planning [12].

MRI is routinely used to assess orbital structures and is preferred to CT because of its limited invasiveness. Volumetric assessment of intra-orbital tissue changes could be helpful for monitoring both disease changes over time and response to treatment. So far few volumetric MRI studies of intra-orbital structures have been published [15-17], and none to our knowledge has included automated assessment of different regions (quadrants) in the orbit.

Our results suggest that the proposed relax-

ometric/geometric semi-automated segmentation approach could be helpful for the quantitative assessment of orbital fat tissue volume. The total fat volume CV for phantom segmentation was below 5%, suggesting our segmentation procedures, ROI definition procedure and post-processing software are accurate and reproducible. The difference in measured versus real volumes could be explained by the partial volume effect between bone and fat at the orbit edges, resulting in underestimation of the orbital fat. The mean percentage operator difference for the results obtained by the two operators with different skill levels showed the robustness of the proposed method, as the results obtained by the operators were similar.

The comparison of fat volumes from patients and controls, using the t test, showed a highly significant separation of the two populations. Moreover, although we used absolute volumes resulting in high CVs (due to the high variability among both patients and controls) significant correlations were found between the amount of fat tissue and both the degree of exophthalmos and the CAS. Taken together, these findings suggest that the proposed method is reliable and potentially useful to assess the disease extent and changes over time. Although our proposed method appears to be reliable and accurate for the estimation of intra-orbital fat, we should still take into account a series of potential limitations. Considering the potential routine clinical application, the method (although far more rapid than fully manual methods) is still time-consuming, requiring up to 10-15 minutes for each study for manual pre-definition of the orbital regions prior to the application of the segmentation procedure. Another limitation is that our segmentation procedure requires two conventional spin echo acquisitions with relatively longer acquisition times than faster magnetic resonance sequences. Finally, although our acquisition procedure used relatively thick slices (3 mm) the measurement accuracy was still acceptable, with strong correlation coefficients and good t test results even for the quadrants considered alone. The method described could be useful for both planning of surgical removal of excess orbital fat and for follow-up studies. Future improvements will relate to the development of a new segmentation strategy based on three-dimensional fast sequences to obtain high-resolution data.

References

1 Tian S, Nishida Y, Isberg B, et al. MRI measurements of normal extra ocular muscles and other orbital structures. Graefes Arch Clin Exp Ophthalmol. 2000; 238: 393-404.
2 Feldon SE, Celina P, Saundra K, et al. Quantitive computer tomography of Graves' ophthalmopathy. Arch Ophtal. 1985; 103: 213-215.
3 Peyster RG, Ginsberg F, Silber JH, et al. Exophthalmos caused by excessive fat: CT volumetric analysis and differential diagnosis. Am J Roentgenol. 1986; 146: 459-464.
4 Nishida Y, Aoki Y, Hayashi O, et al. Volume measurement of horizontal extra ocular muscles with magnetic resonance imaging. Jpn J Ophthalmol. 1996; 40: 439-446.
5 Majos A, Grzelak P, Mynarczyk W, et al. Assessment of the volume of intra-orbital structures using the numerical segmentation image technique (NSI): the extra ocular muscles. Endokrynol Pol. 2007; 58 (2): 110-115.
6 Bartalena L, Pinchera A, Marcocci C. Management of Graves' ophthalmopathy: reality and perspective. Endocr Rev. 2000; 21: 168-199.
7 Weetman A, Cohen SL, Gatter KC, et al. Immunohistochemical analysis of the retrobulbar tissues in Graves' ophthalmopathy. Clin Exp Immunol. 1989; 75: 222-227.
8 Grubeck-Loebenstein B, Treib K, Sztankay A, et al. Retrobulbar T cells from patients with Graves' ophthalmopathy are CD8 and specifically recognize autologous fibroblasts. J Clin Invest. 1994; 93: 2738-2743.
9 Heufelder A, Herterich S, Ernst G, et al. Analysis of retro orbital T cell antigen receptor variable region gene usage in patients with Graves' ophthalmopathy. Eur J Endocrinol. 1995; 132: 266-277.
10 Bartley G, Fatourechi V, Kadrmas EF, et al. Clinical features of Graves' ophthalmopathy in an incidence cohort. Am J Ophthalmol. 1996; 121: 284-290.
11 Feldon SE, Lee CP, Muramatsu SK, et al. Quantitative computed tomography of Graves' ophthalmopathy. Extra ocular muscle and orbital fat in development of optic neuropathy. Archives of Ophthalmology. 1985; 103 (2): 213-215.
12 Boboridis KG, Gogakos A, Krassas GE. Orbital fat decompression for Graves' orbitopathy: a literature review. Pediatr Endocrinol Rev. 2010; 7, Suppl 2: 222-226.
13 Alfano B, Comerci M, Larobina M, et al. An MRI digital brain phantom for validation of segmentation methods. Med Image Anal. 2011; 15 (3): 329-339.
14 Alfano B, Brunetti A, Covelli EM, et al. Unsupervised, automated segmentation of the normal brain using a multispectral relaxometric magnetic resonance approach. Magn. Reson. Med. 1997; 37: 84-93.
15 Nishida Y, Tian S, Isberg B, et al. Significance of orbital fatty tissue for exophthalmos in thyroid-associated ophthalmopathy. Graefes Arch Clin Exp Ophthalmol. 2002; 240: 515-520.
16 Nishida Y, Tian S, Isberg B, et al. MRI measurements of orbital tissues in dysthyroid ophthalmopathy. Graefes Arch Clin Exp Ophthalmol. 2001; 239: 824-831.
17 Prummel MF, Gerding MN, Zonneveld FW, et al. The usefulness of quantitative orbital magnetic resonance imaging in Graves' ophthalmopathy. Clin Endocrinol (Oxf). 2001; 54 (2): 205-209.
18 Dolman PJ, Cahill K, Czyz CN, et al. Reliability of estimating ductions in thyroid eye disease: an International Thyroid Eye Disease Society multicenter study. Ophthalmology. 2012; 119 (2): 382-389.
19 Ossoinig KC. The role of standardized ophthalmic echography in the management of Graves' ophthalmopathy. Dev Ophthalmol. 1989; 20: 28-37.
20 Feldon SE, Weiner JM. Clinical significance of extraocular muscle volumes in Graves' ophthalmopathy. A quantitative computed tomography study. Arch Ophthalmol. 1982; 100 (8): 1266-1269.
21 Matsuo H, Motomura M, Takeo G, et al. Magnetic resonance imaging in diagnosis and follow-up of minimal thyroid ophthalmopathy. Jpn J Med. 1991; 30 (3): 229-232.
22 Feldon SE, Lee CP, Muramatsu SK, et al. Quantitative computed tomography of Graves' ophthalmopathy. Extra ocular muscle and orbital fat in development of optic neuropathy. Arch Ophthalmol. 1985; 103 (2): 213-215.
23 Nishida Y, Tian S, Isberg B, et al. MRI measurements of orbital tissues in dysthyroid ophthalmopathy. Graefes Arch Clin Exp Ophthalmol. 2001; 239 (11): 824-831.
24 Peyster RG, Ginsberg F, Silber JH, et al. Exophthalmos caused by excessive fat: CT volumetric analysis and differential diagnosis. Am J Roentgenol. 1986; 146 (3): 459-464.
25 Bahn RS. Clinical review 157: Pathophysiology of Graves' ophthalmopathy: the cycle of disease. J Clin Endocrinol Metab. 2003; 88 (5): 1939-1946.
26 Ben Simon GJ, Schwarcz RM, Mansury AM, et al. Minimally invasive orbital decompression: local anesthesia and hand-carved bone. Arch Ophthalmol. 2005; 123 (12): 1671-1675.
27 Chang M, Baek S, Lee TS. Long-term outcomes of unilateral orbital fat decompression for thyroid eye disease. Graefes Arch Clin Exp Ophthalmol. 2013; 251 (3): 935-939.
28 Strianese D, Piscopo R, Elefante A, et al. Unilateral proptosis in thyroid eye disease with subsequent contralateral involvement: retrospective follow-up study. BMC Ophthalmol. 2013; 30: 13-21.

Marco Comerci, MD
Istituto di Biostrutture e Bioimmagini
Via De Amicis, 95
80145 Naples, Italy
Tel.: +39 0812203187 - 223
Mobile: +39 3423124621
Fax: +39 0812296117
E-mail: marco.comerci@ibb.cnr.it